PUBLICATIONS OF THE ASTRONOMICAL SOCIETY OF THE PACIFIC, 111:801–808, 1999 July

The Nuclear Spectral Energy Distribution of NGC 4395, the Least Luminous Type 1 Seyfert Galaxy

EDWARD C. MORAN,[1,2] ALEXEI V. FILIPPENKO,[2] LUIS C. HO,[3] JOSEPH C. SHIELDS,[4] TOMASO BELLONI,[5] ANDREA COMASTRI,[6] STEVEN L. SNOWDEN,[7] AND RICHARD A. SRAMEK[8]

Received 1999 March 5; accepted 1999 April 6

ABSTRACT. We present X-ray (*ROSAT*), infrared, and radio observations of NGC 4395, which harbors the optically least luminous type 1 Seyfert nucleus discovered thus far. In combination with published optical and ultraviolet spectra, we have used these data to assemble the broadband spectral energy distribution (SED) of the galaxy's nucleus. Interestingly, the SED of NGC 4395 differs markedly from the SEDs of both quasars and typical low-luminosity active galactic nuclei, which may be a manifestation of the different physical conditions (i.e., black hole masses, accretion rates, and/or accretion modes) that exist in these objects. The nuclear X-ray source in NGC 4395 is variable and has an observed luminosity of just $\sim 10^{38}$ ergs s^{-1}. Although this emission could plausibly be associated with either weak Seyfert activity or a bright stellar-mass binary system, the galaxy's optical and ultraviolet emission-line properties strongly suggest that the X-rays arise from a classical active galactic nucleus.

1. INTRODUCTION

Toward the conclusion of a large survey aimed at quantifying the faint end of the luminosity function of active galactic nuclei (AGNs), Filippenko & Sargent (1989) discovered an extremely low luminosity type 1 Seyfert nucleus in the nearby dwarf galaxy NGC 4395. With an absolute B magnitude of about -10, the AGN in NGC 4395 is some 10^8 times weaker than the most luminous known quasars. Nevertheless, spectroscopy in the optical and ultraviolet bands has indicated that this feeble object is similar to classical type 1 Seyfert galaxies and QSOs in many respects (Filippenko & Sargent 1989; Filippenko, Ho, & Sargent 1993; Filippenko & Ho 1999). For example, the equivalent widths of the broad optical emission lines are typical of type 1 Seyfert galaxies, and the optical/UV continuum is nearly featureless, showing little evidence for stellar absorption lines. In addition, the narrow emission lines span a wide range of ionization from [O I] to [Fe X]; as in other AGNs, these lines probably arise from gas that has been photoionized by a reasonably hard nonstellar continuum (Kraemer et al. 1999).

In this paper we reexamine NGC 4395 in the context of its more luminous counterparts through a comparison of their radio–to–X-ray spectral energy distributions (SEDs). The SEDs of AGNs have, in principle, the power to reveal detailed information about the accretion processes occurring within them. For quasars, which can dominate the total output of their host galaxies at all wavelengths, measurement of the SED is usually straightforward. The SEDs of lower luminosity AGNs, however, can be significantly compromised by contamination from extranuclear sources. In order to minimize this contamination, the SEDs of these objects should be constructed from observations of the highest possible angular resolution (e.g., Ho 1999a). Bearing this in mind, we have assembled the nuclear SED of NGC 4395 between 1.4 GHz and 2 keV using data that have, at most wavelengths, arcsecond-scale resolution. Direct comparison of this SED with the SEDs of quasars and typical low-luminosity AGNs offers valuable insight into the nature of the nuclear activity in NGC 4395.

2. MULTIWAVELENGTH DATA

2.1. Soft X-Ray Observations

NGC 4395 was the target of a 17050 s observation in the 0.1–2.4 keV energy range with the Position Sensitive Proportional Counter (PSPC) on board *ROSAT*. A description

[1] Chandra Fellow.
[2] Department of Astronomy, University of California, Berkeley, CA 94720-3411; edhead@jester.berkeley.edu.
[3] Carnegie Observatories, 813 Santa Barbara Street, Pasadena, CA 91101-1292
[4] Physics and Astronomy Department, Ohio University, Athens, OH 45701-2979.
[5] University of Amsterdam, Kruislaan 403, NL-1098 Amsterdam, The Netherlands.
[6] Osservatorio Astronomico di Bologna, via Zamboni 33, I-40126, Bologna, Italy.
[7] Code 662, NASA Goddard Space Flight Center, Greenbelt, MD 20771.
[8] NRAO, P.O. Box O, Socorro, NM 87801.

of the satellite and X-ray detector are given by Trümper (1983) and Pfeffermann et al. (1986). The observation produced two data sets, an 8007 s exposure collected between 1992 June 2 and June 11 UT and a 9043 s exposure collected between 1992 June 17 and June 19 UT. As Figure 1 indicates, five X-ray sources were detected within 3′ of the nucleus of NGC 4395. One of them (source A), at $\alpha_{2000} = 12^{h}25^{m}48^{s}.6$, $\delta_{2000} = +33°32'51''$, is centered just 4″ from the optical position of the nucleus (McCall, Rybski, & Shields 1985), well within the 1 σ position error radius for on-axis PSPC sources. The radial profile of source A is consistent with that of a point source. None of the other X-ray sources, including the weak source 48″ south of the nucleus (source B), corresponds with an optical feature in the galaxy.

NGC 4395 was also observed with the *ROSAT* High Resolution Imager (HRI) for 11,353 s on 1996 June 23–24 UT. With ∼5″ angular resolution, the HRI allows source positions and spatial extents to be measured with greater accuracy than can be achieved with the ∼30″ resolution afforded by the PSPC. Unfortunately, the nuclear X-ray source in NGC 4395 was not detected in the HRI observation. We have, however, used the HRI data to evaluate the astrometric quality of the PSPC image. Comparing the HRI image to the Palomar Observatory Sky Survey, we find four HRI sources to have optical counterparts within 3″–9″. Each of these sources was detected in the PSPC image at positions that closely match their HRI positions. Thus, we are confident that source A in Figure 1 is indeed coincident with the nucleus of NGC 4395.

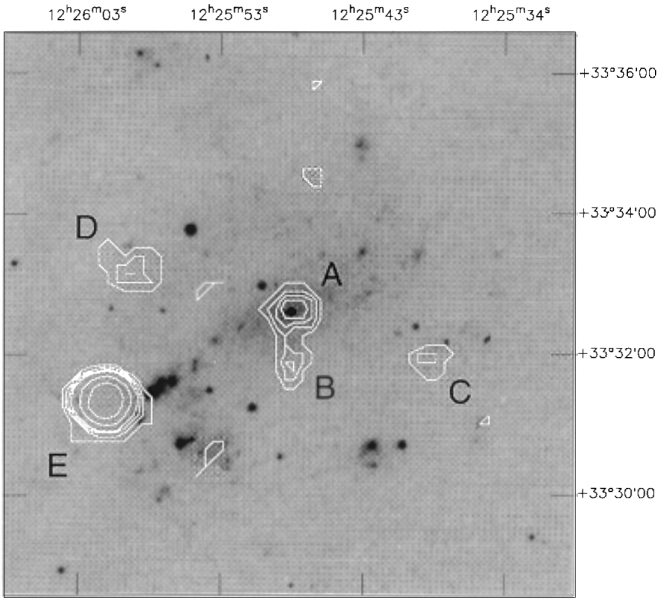

FIG. 1.—Contours from the *ROSAT* PSPC image of NGC 4395 overlaid on an 8′ × 8′ optical image from the Digitized Sky Survey. The PSPC image was smoothed with a $\sigma_G = 7''$ Gaussian. The contours represent intensity levels of 2, 3, 4, 5, 9, 16, and 31 (smoothed) counts per pixel. Source A is coincident with the optical nucleus of NGC 4395. None of the other sources detected appears to correspond to an optical feature. As a result of the smoothing, source B appears to be partially merged with the nuclear X-ray source; the two sources are well resolved in the raw X-ray image. The ordinate (declination) and abscissa (right ascension) are labeled with J2000 coordinates.

For spectral and temporal analysis of source A, we extracted PSPC counts within a 38″ radius circle, which we offset a few arcseconds to the north of the nucleus of NGC 4395 to minimize the possible contamination from source B. A total of 157 counts were detected in this region. Using the documented characteristics of the *ROSAT* PSPC on-axis point-spread function (Hasinger et al. 1992), we calculate that no more than two of these counts could arise from source B, assuming it is spatially unresolved. To estimate the sky background, we collected counts within an annulus centered on the nucleus with inner and outer radii of 4′ and 5.′25, respectively. This region excludes the other sources shown in Figure 1 but is close enough to the optical axis that we may neglect vignetting effects. Scaling the number of counts in the annulus to the area of the source region implies a background level of 37 counts in the source region. Thus, the significance of the detection of the nucleus of NGC 4395 is 9.6 σ, and the net count rate of the source, averaged over the entire observation, is $(7.0 \pm 0.7) \times 10^{-3}$ counts s^{-1}. For spectral fitting, we rebinned the PSPC spectrum to have a minimum of 20 counts (source plus background) per channel. With the exception of the lowest energy channel, each spectral bin has a signal-to-noise ratio of at least 3.

An independent analysis of the *ROSAT* data for NGC 4395 has been carried out recently by Lira et al. (1999). Although some of their findings are qualitatively similar to those we describe below, our analysis methods and quantitative results differ in detail. In particular, the PSPC count rate derived by Lira et al. is higher than ours, probably due to contamination by source B in their large extraction aperture.

2.1.1. The Soft X-Ray Spectrum

With just 120 source photons, only a limited investigation of the soft X-ray spectral characteristics of NGC 4395 is possible. Therefore, we have applied only simple, single-component models to the PSPC spectrum. An absorbed power-law model ($F_E \propto E^{-\alpha}$), which is frequently employed in AGN studies, yields the following best-fit spectral parameters: a very flat power-law energy index of $\alpha \approx -0.1$, and an absorption column density of $N_H = 1.6 \times 10^{20}$ cm^{-2}, which is consistent with the value of the Galactic neutral hydrogen column in the direction of NGC 4395 (1.43×10^{20} cm^{-2}; Murphy et al. 1996). We were surprised to find that, despite the limited statistics of the source counts, the fit afforded by the power-law model is formally unacceptable; with N_H fixed at the Galactic column density,

$\chi^2 = 10.9$ for 4 degrees of freedom. Very similar results were obtained using a different background region, so we are confident that the poorness of the power-law fit is not an artifact of the background subtraction. Fits involving single-component thermal models or an intrinsically steep, but heavily absorbed, power law proved to be inadequate as well. As Figure 2 illustrates, the residuals from the best power-law fit exhibit a systematic S-shaped wiggle, which may signify the presence of complex features (i.e., multiple absorption or emission components) in the soft X-ray spectrum. Unfortunately, the quality of the PSPC data is insufficient for a direct investigation of this possibility. The power-law fit is, however, adequate for the construction of the nuclear SED of NGC 4395, and we use it below for that purpose.

2.1.2. X-Ray Variability

As noted above, the PSPC observation of NGC 4395 was divided into two segments approximately equal in exposure and spaced by about 12 days. Although the overall statistics are too poor to allow the production of a proper light curve, we have looked for possible variability of the nuclear X-ray source between these segments. To do this, we extracted source and background counts for each data set individually using the procedure described above. We find that while the background did not vary between the two observations, the nucleus of NGC 4395 did. We measure a source count rate for the first interval (8007 s) of $(3.7 \pm 0.9) \times 10^{-3}$ counts s^{-1}. During the second interval (9043 s), the source count rate increased to $(10.0 \pm 1.2) \times 10^{-3}$ counts s^{-1}. Thus, the nucleus of NGC 4395 varied by a factor of ~ 3 (significant at the 4.3 σ level) on this short timescale. For comparison, we examined other sources in the field for variability; the count rate of source E in Figure 1 increased by 30% between the two observations (2.7 σ significance), while that of a source $\sim 8'$ to the southwest of NGC 4395 (not shown in Fig. 1) decreased by 12% (0.8 σ significance).

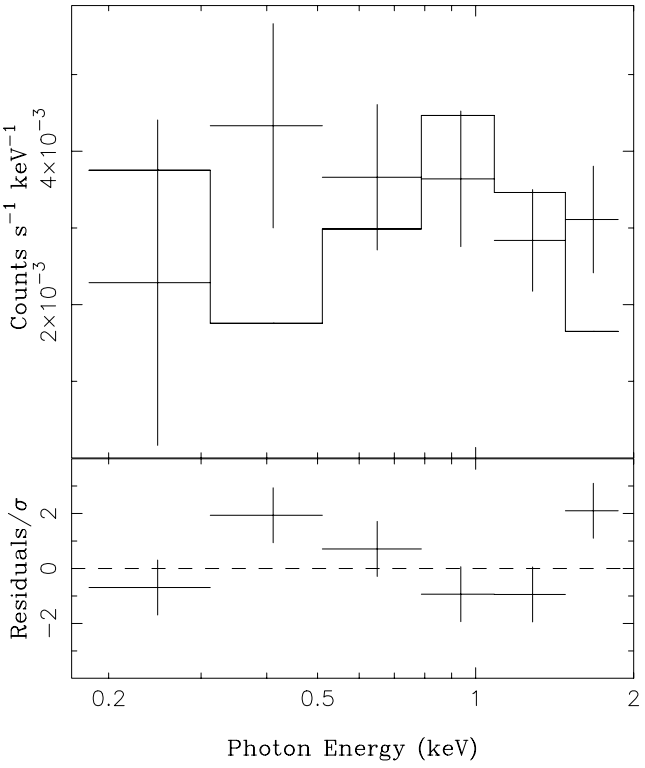

FIG. 2.—The *ROSAT* PSPC counts spectrum of NGC 4395, fitted with the absorbed power-law model described in the text. The systematic, rather than random, displacement of the fit residuals suggests that the spectrum possesses complex features.

Variability explains why the nuclear X-ray source in NGC 4395 was not detected by the HRI. We measure a 3 σ upper limit of 1.0×10^{-3} counts s^{-1} for the HRI count rate of this source. Assuming the spectral parameters obtained for the power-law model in the previous section, this limit corresponds to a PSPC count rate of 2.9×10^{-3} counts s^{-1}, which is even less than the source's "low state" during the PSPC observation.

We have examined the PSPC data to see if the count-rate variability of the nuclear X-ray source in NGC 4395 was accompanied by spectral variations. As a crude means of investigating this issue, we have measured the "hardness ratio" of the source in both segments of the PSPC observation. The hardness ratio is defined in the following manner: $HR = (H - S)/(H + S)$, where H and S represent the number of source counts detected in "hard" (0.94–2.4 keV) and "soft" (0.1–0.94 keV) bands of the spectrum. The demarcation energy of 0.94 keV divides the *total* PSPC counts detected from the nucleus equally into the two bands (i.e., HR = 0.0 for the full 17 ks observation). We measure $HR = -0.13 \pm 0.21$ for the first segment of the observation and $HR = +0.04 \pm 0.12$ for the second. Although the uncertainties are substantial, these results are consistent with there being no spectral variability in conjunction with the intensity variations of the nuclear X-ray source.

The issue of hardness ratio variability provides further insight into the nature of the soft X-ray spectrum of NGC 4395. There are two commonly observed types of AGN spectra that might account for the S-shaped pattern in the residuals seen in Figure 2. The first of these consists of two emission components: a thermal component that dominates at the softest X-ray energies and a moderately absorbed nonthermal component that contributes mainly at higher energies. Spectra of this form have been successfully used to model the broadband X-ray emission of other low-luminosity AGNs (Serlemitsos, Ptak, & Yaqoob 1996). The second type of model consists of a single power-law component that is absorbed by both neutral and ionized material. The signatures of ionized ("warm") absorption are often observed in the spectra of luminous

type 1 Seyfert galaxies (e.g., Reynolds 1997). In the two-component model, the thermal emission is presumed to be spatially extended, so it should not vary on short timescales. Thus, in this picture, we might expect strong hardness ratio variability to accompany the intensity variations observed in NGC 4395. The absence of significant changes in the hardness of the spectrum suggests instead that only one emission component is present, which favors the warm absorber scenario.

2.2. Ultraviolet and Optical Spectroscopy

Our investigation of the spectral energy distribution of NGC 4395 includes published ultraviolet and optical spectra from Filippenko et al. (1993) and Kraemer et al. (1999), which provide a full description of the acquisition, reduction, and analyses of the data. The salient details of these spectra are summarized as follows. The UV spectrum was acquired with the Faint Object Spectrograph on board the *Hubble Space Telescope* (prerefurbishment) through an effective aperture of $1\farcs4 \times 4\farcs3$; it covers the 1150–3300 Å range at a resolution of 1.2–3.3 Å. The ground-based optical spectrum, which covers the 3200–10000 Å range at a resolution of 5–8 Å, was acquired under photometric conditions with $\sim 1''$ seeing and a $2'' \times 4''$ aperture.

Extinction by dust in NGC 4395, if present, could affect the shape of the galaxy's optical/UV spectrum and its apparent luminosity. Because NGC 4395 is a face-on, bulgeless, low-metallicity spiral, extinction in the nucleus is expected to be very low. This is, in fact, what both optical emission-line flux ratio measurements (Ho, Filippenko, & Sargent 1997) and our power-law fit to the *ROSAT* PSPC spectrum (§ 2.1.1) suggest. But this evidence should be interpreted cautiously: the emission-line flux ratios reflect the amount of extinction between us and the galaxy's narrow-line region, not its continuum source, and as we have noted, a power law may not describe the spectrum of the nuclear X-ray emission accurately. As discussed in § 3, there is indirect evidence that the far-UV continuum of NGC 4395 is absorbed. In addition, our UV spectrum exhibits an abrupt inflection near 2200 Å (Filippenko et al. 1993); this is approximately coincident with the strong 2175 Å bump in the Galactic reddening law, which could indicate the presence of dust. In an attempt to constrain the extinction in NGC 4395, we have applied the Galactic reddening law of Cardelli, Clayton, & Mathis (1989) using a range of values for the equivalent V-band absorption A_V. For A_V in excess of 0.2 mag, we find that the 2175 Å feature is overcorrected. Although this procedure for constraining A_V can be very uncertain (see Fitzpatrick 1999), it nonetheless provides a practical upper limit to the amount of extinction in the nucleus of NGC 4395. But since there is no compelling evidence for extinction intrinsic to NGC 4395, we correct only for Galactic reddening when constructing the SED.

It has been recently reported that the shape of the optical continuum of NGC 4395 undergoes dramatic changes on timescales as short as 6 months (Lira et al. 1999). As we have been monitoring NGC 4395 for many years, we are able to investigate this claim independently. Figure 3 shows five of our broadband optical spectra, which were acquired and reduced in the same manner as the data described above. Accompanying each spectrum is a set of dotted lines that approximate the three "states" observed by Lira et al. (1999) over the same wavelength range. As the dates listed in Figure 3 indicate, our spectra cover a variety of time baselines ranging from 2 months to almost 4 years. Qualitatively, the spectra all have the same general appearance: none can be described as a power law, and all are concave downward. Although there appear to be some differences

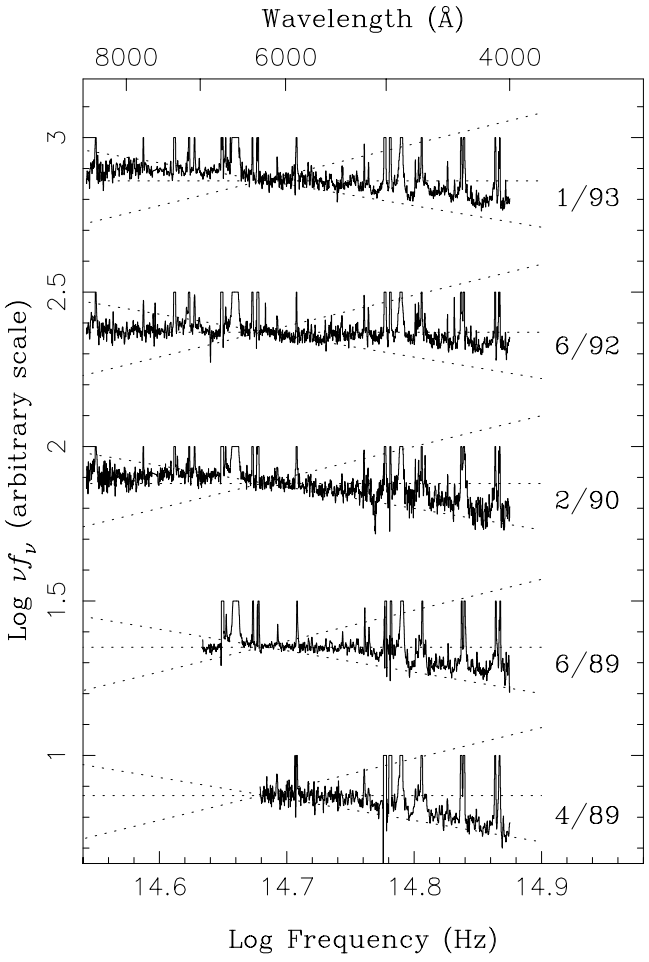

FIG. 3.—Five optical spectra of NGC 4395, obtained over a ~4 year period at Lick Observatory. The strong emission lines in the spectra have been truncated to emphasize the shape of the continuum. The dotted lines, normalized to intersect the spectrum of NGC 4395 near a wavelength of 6300 Å, approximate the various spectral states observed by Lira et al. (1999) over the same wavelength range. While there are some differences among our spectra, we do not see evidence for the extreme spectral variability claimed by Lira et al. (1999).

between the spectra, we do not see evidence for the extreme spectral variability reported by Lira et al. (1999). Moreover, the differences we observe may be caused, in part, by minor inconsistencies in our flux calibration and extinction correction procedures. Unfiltered images of NGC 4395 obtained at five epochs spanning 40 days with the Katzman Automatic Imaging Telescope (KAIT; Treffers et al. 1997) do indicate that the nucleus is variable by at least 0.25 mag. Thus, we have initiated a *BVRI* monitoring campaign in order to search for color variability. We note, however, that the "low state" observed by Lira et al. (1999), if real, cannot be very common in NGC 4395; otherwise, the UV/optical spectrum would be characterized by low-ionization emission lines, such as those in LINERs (Ho, Filippenko, & Sargent 1993), rather than the high-ionization lines that are consistently observed in the spectrum. Perhaps the "low state" spectrum was adversely affected by nongray particles in the Saharan dust mentioned by Lira et al.

2.3. Infrared Observations

Infrared images of the NGC 4395 nucleus were obtained using the Near-Infrared Camera (Matthews & Soifer 1994) on the Keck I 10 m telescope on 1995 January 20 UT. Five exposures with integration times of 45, 25, and 25 s were acquired in each of the J, H, and K bandpasses, respectively. The seeing during these observations ranged from approximately 0.″5 (FWHM) in K to 0.″7 in J. Fluxes were measured within a 1.″5 radius aperture, and the standard star G163−50 (Casali & Hawarden 1992) was used for absolute flux calibration. The following magnitudes and 1 σ errors were derived: $J = 15.58 \pm 0.06$ mag, $H = 14.98 \pm 0.05$ mag, and $K = 14.35 \pm 0.06$ mag. While these magnitudes are dominated by the nuclear point source, some very low level contamination from faint circumnuclear starlight may be present.

We have measured the strength of the continuum of NGC 4395 at 3.94 μm, based on an 18.6 ks observation with the Short Wavelength Spectrometer (SWS) on board the *Infrared Space Observatory*.[9] Full details of the observation and data reduction are provided in Kraemer et al. (1999). The 3.9 μm flux density of NGC 4395 is 6.7 ± 0.7 mJy, after removal of the estimated background of 0.7 mJy due to zodiacal emission. Based on analysis of our K-band image, we estimate further that $\sim$30% of this flux arises from extranuclear sources in the 14″ × 20″ SWS aperture; applying this correction, we derive a 3.9 μm flux density of 4.7 ± 0.7 mJy for the nucleus.

NGC 4395 has also been observed in the N band by Maiolino et al. (1995), who report a 10 μm flux density of 12 ± 3.9 mJy. A 5.″3 diameter aperture was employed in this observation, so a small contribution from the galaxy may be present in this measurement as well.

2.4. Radio Observations

Radio continuum observations of NGC 4395 were made at a wavelength of 20 cm on 1990 March 3 with the NRAO[10] Very Large Array (VLA), which was operated in the high-resolution A configuration. The on-source integration was about 8 hr. Phase calibration was performed using the nearby unresolved source 1219+285, and 3C 286 was used to establish the amplitude scale. The rms noise level in the 20 cm image, which was presented previously by Sramek (1992), is 0.036 mJy. We also analyzed an archived 6 cm VLA A-array observation of NGC 4395 from 1982 February 8. The rms noise level in the 6 cm map is 0.12 mJy. Both radio images were convolved to a beam size of 2.″7; at this resolution, the nuclear radio source in NGC 4395 is spatially unresolved. After applying corrections for primary beam attenuation (0.87 at 6 cm) and attenuation due to bandwidth effects (0.84 at 20 cm and 0.90 at 6 cm), we obtain the following source flux densities: $S_{20} = 1.24 \pm 0.07$ mJy and $S_6 = 0.56 \pm 0.12$ mJy. The uncertainties include a 5% calibration error contribution. For a power-law spectrum of the form $S_\nu \propto \nu^{-\alpha}$, these flux densities imply a radio spectral index[11] of $\alpha = 0.66 \pm 0.22$.

3. THE NUCLEAR SED OF NGC 4395

We have combined the data described in the previous section to construct the observed spectral energy distribution of NGC 4395. The result, plotted in νL_ν units and corrected for Galactic absorption, is displayed in Figure 4*a*. The X-ray region of the SED (0.2–2 keV) is depicted as the power law discussed in § 2.1.1, normalized to be consistent with the average PSPC count rate. Again, this power law provides a reasonable approximation of the observed soft X-ray spectrum, but it is unlikely to be accurate in detail. The dotted line between 3.3×10^{15} and 4.8×10^{16} Hz (i.e., 13.6 and 200 eV) was not measured; we use it below to estimate the ionizing photon luminosity of the nucleus.

We are confident that Figure 4*a* represents the *nuclear* SED of NGC 4395, since it consists mainly of data obtained with resolutions and/or apertures a few arcseconds or less in extent. (For a distance of 2.6 Mpc, 1″ corresponds to 13 pc.)

[9] The *Infrared Space Observatory* is an ESA project with instruments funded by ESA Member States with the participation of ISAS and NASA.

[10] The National Radio Astronomy Observatory is a facility of the National Science Foundation operated under cooperative agreement by Associated Universities, Inc.

[11] Our spectral index measurement assumes that the nuclear radio source in NGC 4395 did not vary between the 6 and 20 cm observations. NGC 4395 was detected in the VLA FIRST survey (White et al. 1997) with a 20 cm flux density of 1.2 mJy, equal to the value we obtained in 1990, suggesting that this assumption is valid.

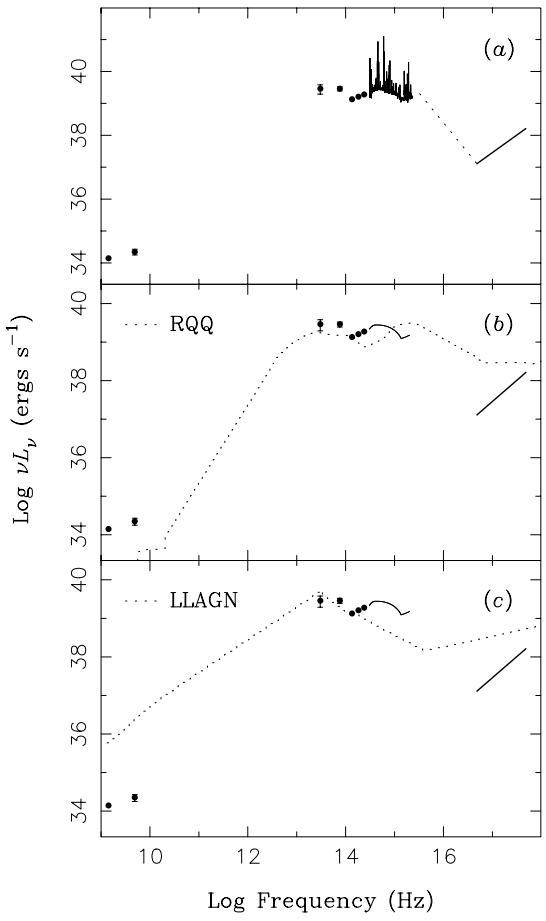

FIG. 4.—(*a*) The nuclear radio–to–X-ray spectral energy distribution of NGC 4395, corrected for Galactic extinction ($A_V = 0.02$ mag). We have not attempted to correct for absorption that may be intrinsic to NGC 4395. As described in the text, we have artificially added the far-UV power law (*dotted line*) between 13.6 and 200 eV. (*b*) Comparison of the SED of NGC 4395 to the median radio-quiet quasar (RQQ) SED (*dotted line*) from Elvis et al. (1994). For clarity, we have replaced the spectrum of NGC 4395 in the optical/UV region with a continuum fit. The quasar SED has been normalized to intersect the SED of NGC 4395 at 2.2 μm. (*c*) The SED of NGC 4395 compared with the median SED of the low-luminosity AGNs (*dotted line*) studied by Ho (1999a). In constructing the median LLAGN SED, we have omitted the optical/UV spectra of two objects (NGC 4261 and NGC 4374) that have heavy amounts of internal reddening. Again, the LLAGN SED has been normalized to intersect the SED of NGC 4395 at 2.2 μm.

The two exceptions—the *ISO* and *ROSAT* measurements—are also very likely to reflect nuclear fluxes. As discussed in § 2.3, we have corrected the *ISO* 3.9 μm flux density for extranuclear contamination. Furthermore, based on our comparison of the *ROSAT* PSPC, *ROSAT* HRI, and optical images of NGC 4395, we have shown that the source of soft X-ray emission identified as source A in Figure 1 is very likely to be associated with the galaxy's nucleus. The amplitude and timescale of the 0.2–2 keV variability implies that the majority of the nuclear soft X-ray emission arises from a very compact region ($r < 0.01$ pc), leaving little room for a significant extranuclear component.

As Figure 4*a* indicates, the nuclear SED of NGC 4395 peaks at least twice, once somewhere in the near-IR band and again in the optical band at $\sim 5 \times 10^{14}$ Hz ($\sim$6000 Å). The SED is also rising in the UV above $\sim 2 \times 10^{15}$ Hz (which is the case even if an extinction correction of $A_V = 0.2$ mag is applied). Integration of the SED[12] yields a bolometric luminosity of $L_{\rm bol} \approx 1.9 \times 10^{40}$ ergs s^{-1} for the nucleus of NGC 4395 (3.2×10^{40} ergs s^{-1} for $A_V = 0.2$ mag), close to the value of 1.5×10^{40} ergs s^{-1} predicted by Filippenko & Sargent (1989) on the basis of the observed broad Hβ line luminosity.

We have used the artificial power law connecting the observed ultraviolet spectrum (extrapolated to 13.6 eV) and the time-averaged soft X-ray spectrum to obtain a conservative estimate of the nuclear ionizing photon luminosity Q. Integration of the SED between 13.6 eV and 2 keV yields $Q_{\rm obs} = 3.1 \times 10^{49}$ photons s^{-1} ($= 5.3 \times 10^{49}$ photons s^{-1} if $A_V = 0.2$ mag). For Case B recombination (Osterbrock 1989), the ionizing photon luminosity required to account for the total observed Hβ luminosity $L(\mathrm{H}\beta) = 4.4 \times 10^{37}$ ergs s^{-1} (Filippenko & Sargent 1989) is $Q_{\rm req} = 9.2 \times 10^{49} f^{-1}$ photons s^{-1}, where f is the combined covering factor of the broad and narrow emission line gas. Although f is unmeasured, it must have a value less than unity; thus, $Q_{\rm obs} < Q_{\rm req}$, which implies a deficit of ionizing radiation for this form of the SED. Since the nuclear X-ray source in NGC 4395 is variable, the galaxy's average ionizing luminosity may be higher than we have estimated it to be. On the other hand, it is unlikely that the fiducial far-UV spectrum we have adopted describes the correct shape of the ionizing continuum. As noted above, the UV portion of the observed SED is rising (in νL_ν) at frequencies greater than $\sim 2 \times 10^{15}$ Hz. Therefore, the actual far-UV spectrum of NGC 4395 probably contains flux in excess of the power law we have assumed. Kraemer et al. (1999) have noted that this power law, which has an energy index of $\alpha \approx 3$ for $F_\nu \propto \nu^{\alpha}$, is far too steep to account for the observed He II/Hβ emission-line flux ratio. Interestingly, the slope $\alpha = 1.7$ needed to explain the He II/Hβ ratio would also be sufficient to eliminate the apparent deficit of Q for $A_V = 0.2$ mag. In any case, the intrinsic 13.6–200 eV spectrum (or a part of it) is almost certainly flatter than indicated in Figure 4*a*, which may signify that the absorption column density in the nucleus of NGC 4395 is larger than suggested by our power-law fit to the PSPC spectrum.

A comparison between the nuclear SED of NGC 4395 and the median SEDs of radio-quiet quasars (compiled by

[12] We have assumed that the continuum can be described as simple power laws over the ranges 5 GHz–10 μm, 10–3.9 μm, 3.9–2.2 μm, and 13.6–200 eV.

Elvis et al. 1994) and typical low-luminosity AGNs (LLAGNs; compiled by Ho 1999a) is provided in Figures 4*b* and 4*c*, respectively. In each plot, the reference SED is shown as a dotted line arbitrarily normalized to the SED of NGC 4395 at 1.36×10^{14} Hz (2.2 μm). For clarity, we have replaced the optical/UV spectrum of NGC 4395 with a continuum fit. The SED of NGC 4395, particularly from the near-IR to the UV, differs dramatically from the SEDs of both quasars and LLAGNs (which, as noted by Ho 1999b, are very different from each other). In NGC 4395, the SED rises in the near-IR and declines in the UV, whereas the quasar SED has a local minimum in the near-IR and rises in the UV. None of this structure is present in the median LLAGN SED, which declines steadily from the near-IR to the far-UV. Relative to the flux density at 2.2 μm, NGC 4395 is a stronger radio source than the typical radio-quiet quasar, but it is not as radio-loud as other LLAGNs. In the far-UV and soft X-ray region, the SED of NGC 4395 also appears to deviate from the quasar and LLAGN SEDs; however, further characterization of the X-ray spectrum and variability of NGC 4395 is required before this conclusion can be drawn.

At this time we are unable to provide a full explanation for the differences between the SEDs of quasars, typical LLAGNs, and NGC 4395, but we offer the following qualitative argument as a starting point for an investigation of the issue. As Blandford & Rees (1992) have discussed, the radiation energy density of an optically thick region a fixed distance (in gravitational radii) from a massive, collapsed object depends only on $M_{\rm BH}$, the mass of the object (assumed here to be a black hole), and $L_{\rm bol}/L_{\rm edd}$, the ratio of the bolometric to Eddington luminosity of the region. It would therefore be of interest to compare $M_{\rm BH}$ and $L_{\rm bol}/L_{\rm edd}$ for quasars, LLAGNs, and NGC 4395. For typical high-luminosity quasars, it is presumed that $M_{\rm BH} > 10^9\ M_\odot$ and $L_{\rm bol}/L_{\rm edd} \approx 10^{-1}$–$10^{-2}$ (e.g., Padovani & Rafanelli 1988; McLure et al. 1999). The majority of the LLAGNs from Ho (1999a) have $M_{\rm BH} \approx 10^6$–$10^9\ M_\odot$ and $L_{\rm bol}/L_{\rm edd} \approx 10^{-4}$–$10^{-6}$. In the case of NGC 4395, the stellar kinematics near the nucleus place an upper limit of $8 \times 10^4\ M_\odot$ for the mass of the central black hole (Filippenko & Ho 1999), which implies $L_{\rm edd} < 1 \times 10^{43}$ ergs s^{-1} and $L_{\rm bol}/L_{\rm edd} > 2 \times 10^{-3}$. The latter limit will be even higher if there is significant extinction in the nucleus of NGC 4395. Clearly, quasars, LLAGNs, and NGC 4395 occupy very different regions in the $M_{\rm BH}$-$L_{\rm bol}/L_{\rm edd}$ plane, which may be partly responsible for the dissimilarity of their SEDs. Of course, there are undoubtedly other important factors to consider. For example, most of the LLAGNs studied by Ho (1999a) are LINERs, which, unlike quasars and luminous Seyfert galaxies, may be powered by advection-dominated accretion flows rather than geometrically thin accretion disks (e.g., Lasota et al. 1996). Further investigation of the broad-band characteristics of active galaxies, particularly those with measured black hole masses, will clarify the relationship between their physical properties and their SEDs.

4. NATURE OF THE NUCLEAR X-RAY SOURCE

The small physical size of the nuclear X-ray source in NGC 4395, deduced from its large-amplitude (300%), short timescale ($\sim$10 days) variability, suggests that this emission results from the accretion of matter onto a massive, compact object. But with a mean observed 0.2–2 keV luminosity of just 1.3×10^{38} ergs s^{-1} (calculated for the $\alpha = -0.1$ power-law spectrum described in § 2.1.1 and a distance of 2.6 Mpc), the physical nature of the accreting object is somewhat unclear. While an AGN could easily account for this modest luminosity, it could also be produced by a single bright binary star system emitting near the Eddington limit for a stellar-mass neutron star or black hole. Some of the luminous X-ray emitters identified recently in the off-nuclear regions of nearby galaxies might be examples of the latter (Colbert & Mushotzky 1999). Both AGNs and X-ray binaries are known to flicker, so the variability of the source does not help to distinguish between the two possibilities. The nuclear X-ray spectrum of NGC 4395, because of its apparent flatness, bears a closer resemblance to the spectra of high-mass X-ray binaries ($\bar{\alpha} \approx 0.2$; White, Swank, & Holt 1983) than to those of luminous broad-line AGNs ($\bar{\alpha} \approx 1.5$ in the *ROSAT* band; Walter & Fink 1993), which might be cited as support for the binary hypothesis. However, as we have discussed above, this spectrum probably possesses complex features, so conclusions regarding its true shape must be deferred until high-resolution broad-band observations from *Chandra* become available. High-mass X-ray binaries emit most of their luminosity in the X-ray band, so if the nuclear X-ray source were a binary star system, the slope of the galaxy's far-UV spectrum would have to be even *steeper* than it is shown to be in Figure 4*a*. This circumstance is firmly ruled out by the observed strength of the He II/Hβ optical emission-line flux ratio (Kraemer et al. 1999). Thus, despite the scarcity of direct evidence linking the nuclear X-ray emission in NGC 4395 to an AGN, we feel that it is very likely to be associated with the object responsible for the galaxy's optical and UV emission-line properties. Some of the off-nuclear X-ray sources shown in Figure 1, however, could be luminous X-ray binaries or supernova remnants, as discussed by Colbert & Mushotzky (1999).

5. SUMMARY

We have presented the nuclear radio–to–X-ray spectral energy distribution of NGC 4395, the least luminous broad-line Seyfert galaxy currently known. While this object exhibits many of the characteristics of its more luminous counterparts, its SED differs markedly. Interestingly, the

SED of NGC 4395 does not resemble the SEDs of other (predominantly LINER) low-luminosity AGNs either, which themselves differ from the typical quasar SED. The full reason for the dissimilarity between these SEDs is uncertain. We have noted, however, that NGC 4395, quasars, and LLAGNs have different combinations of black hole mass and Eddington-normalized bolometric luminosity, which may be a significant factor. Continued broadband study of AGNs of all spectroscopic classes and luminosities is needed to elucidate the connection between the shape of their SEDs and their physical attributes.

The *ROSAT* data discussed here represent the first detection of X-ray emission from the nucleus of NGC 4395. Although weak, the nuclear X-ray source exhibits large-amplitude variability on short timescales and has an apparently flat soft X-ray spectrum. A simple absorbed power-law model, however, does not provide an acceptable fit to this spectrum; we speculate that the spectrum may contain additional emission or absorption components. There may be some ambiguity about the origin of the nuclear X-ray emission because of its faintness, but we have argued that if it were associated with anything other than an AGN, it would be very difficult (or impossible) for NGC 4395 to power the Seyfert-like emission lines observed in the optical and UV portions of its spectrum. *Chandra* observations should clarify the nature of this source.

We would like to express our thanks to Kirk Korista, the referee, for his thoughtful comments on the manuscript. We are also grateful to M. Eracleous for helpful discussions, to D. DePoy, J. Graham, W. Harrison, and M. Liu for assistance with the Keck observations and data analysis, and to W. Li and M. Papenkova for providing the KAIT magnitude measurements. Support for this work was provided by NASA through grants NAG5-3556, NAG5-3563, NAG5-3690, and AR-07527 (through STScI, which is operated by AURA, Inc., under NASA contract NAS5-26555). E. C. M. acknowledges partial support by NASA through Chandra Fellowship grant PF8-10004 awarded by the Chandra X-Ray Center, which is operated by the Smithsonian Astrophysical Observatory for NASA under contract NAS8-39073. The W. M. Keck Observatory is operated as a scientific partnership between the California Institute of Technology, the University of California, and NASA, and was made possible by the generous financial support of the W. M. Keck Foundation.

REFERENCES

Blandford, R. D., & Rees, M. J. 1992, in Testing the AGN Paradigm, ed. S. S. Holt, S. G. Neff, & C. M. Urry (New York: AIP), 3
Cardelli, J. A., Clayton, G. C., & Mathis, J. S. 1989, ApJ, 345, 245
Casali, M. M., & Hawarden, T. G. 1992, JCMT-UKIRT Newsl., 3, 33
Colbert, E. J. M., & Mushotzky, R. F. 1999, ApJ, 519, 89
Elvis, M., et al. 1994, ApJS, 95, 1
Filippenko, A. V., & Ho, L. C. 1999, ApJ, submitted
Filippenko, A. V., Ho, L. C., & Sargent, W. L. W. 1993, ApJ, 410, L75
Filippenko, A. V., & Sargent, W. L. W. 1989, ApJ, 342, L11
Fitzpatrick, E. L. 1999, PASP, 111, 63
Hasinger, G., Turner, T. J., George, I. M., & Boese, G. 1992, Legacy, 2, 77
Ho, L. C. 1999a, ApJ, 516, 672
———. 1999b, in The AGN-Galaxy Connection, ed. H. R. Schmitt, L. C. Ho, & A. L. Kinney, Adv. Space Res., in press (astro-ph/9807273)
Ho, L. C., Filippenko, A. V., & Sargent, W. L. W. 1993, ApJ, 417, 63
———. 1997, ApJS, 112, 315
Kraemer, S. B., Ho, L. C., Crenshaw, D. M., Shields, J. C., & Filippenko, A. V. 1999, ApJ, in press
Lasota, J.-P., Abramowicz, M. A., Chen, X., Krolik, J., Narayan, R., & Yi, I. 1996, ApJ, 462, 142
Lira, P., Lawrence, A., O'Brien, P., Johnson, R. A., Terlevich, R., & Bannister, N. 1999, MNRAS, in press
Maiolino, R., Ruiz, M., Rieke, G. H., & Keller, L. D. 1995, ApJ, 446, 561
Matthews, K., & Soifer, B. T. 1994, in Infrared Astronomy with Arrays: The Next Generation, ed. I. McLean (Dordrecht: Kluwer), 239
McCall, M. L., Rybski, P. M., & Shields, G. A. 1985, ApJS, 57, 1
McLure, R. J., Dunlop, J. S., Kukula, M. J., Baum, S. A., O'Dea, C. P., & Hughes, D. J. 1999, ApJ, in press
Murphy, E. M., Lockman, F. J., Laor, A., & Elvis, M. 1996, ApJS, 105, 365
Osterbrock, D. E. 1989, Astrophysics of Gaseous Nebulae and Active Galactic Nuclei (Mill Valley: Univ. Sci. Books)
Padovani, P., & Rafanelli, P. 1988, A&A, 205, 53
Pfeffermann, E., et al. 1986, Proc. SPIE, 733, 519
Reynolds, C. S. 1997, MNRAS, 286, 513
Serlemitsos, P., Ptak, A., & Yaqoob, T. 1996, in ASP Conf. Ser. 103, The Physics of LINERs in View of Recent Observations, ed. M. Eracleous, A. Koratkar, C. Leitherer, & L. Ho (San Francisco: ASP), 70
Sramek, R. 1992, in ASP Conf. Ser. 31, Relationships between Active Galactic Nuclei and Starburst Galaxies, ed. A. V. Filippenko (San Francisco: ASP), 273
Treffers, R. R., Peng, C. Y., Filippenko, A. V., & Richmond, M. W. 1997, IAU Circ. 6627
Trümper, J. 1983, Adv. Space Res., 2(4), 241
Walter, R., & Fink, H. H. 1993, A&A, 274, 105
White, N., Swank, J., & Holt, S. 1983, ApJ, 270, 711
White, R. L., Becker, R. H., Helfand, D. J., & Gregg, M. D. 1997, ApJ, 475, 479